NonDestructive Positron Plasma Diagnostics for Antihydrogen Production

M. Amoretti, C. Amsler, G. Bonomi, A. Bouchta, P. D. Bowe, C. Carraro, C. L. Cesar, M. Charlton, M. Doser, V. Filippini, A. Fontana, M. C. Fujiwara, R. Funakoshi, P. Genova, J. S. Hangst, R. S. Hayano, L. V. Jo/rgensen, V. Lagomarsino, R. Landua, D. Lindelöf, E. Lodi Rizzini, M. Macri, N. Madsen, G. Manuzio, P. Montagna, H. Pruys, C. Regenfus, A. Rotondi, G. Testera, A. Variola, D. P. van der Werf, R. L. Spencer, and ATHENA Collaboration

Articles you may be interested in
Antihydrogen formation from antiprotons in a pure positron plasma
Phys. Plasmas **16**, 012101 (2009); 10.1063/1.3040168

Analysis of time-dependent effects when operating nested-well plasma traps for achieving antihydrogen recombination
AIP Conf. Proc. **498**, 71 (1999); 10.1063/1.1302103

Self-consistent static analysis of using nested-well plasma traps for achieving antihydrogen recombination
AIP Conf. Proc. **498**, 65 (1999); 10.1063/1.1302102

Development and testing of a positron accumulator for antihydrogen production
AIP Conf. Proc. **498**, 13 (1999); 10.1063/1.1302096

Progress in creating low-energy positron plasmas and beams
AIP Conf. Proc. **498**, 3 (1999); 10.1063/1.1302095

Non-Destructive Positron Plasma Diagnostics for Antihydrogen Production

M. Amoretti[1],[*], C. Amsler[†], G. Bonomi[**], A. Bouchta[**], P. D. Bowe[‡],
C. Carraro[*], C. L. Cesar[§], M. Charlton[‡], M. Doser[**], V. Filippini[¶],
A. Fontana[¶], M. C. Fujiwara[‖], R. Funakoshi[‖], P. Genova[¶], J. S. Hangst[††],
R. S. Hayano[‖], L. V. Jørgensen[‡], V. Lagomarsino[*], R. Landua[**],
D. Lindelöf[†], E. Lodi Rizzini[‡‡], M. Macri[*], N. Madsen[††], G. Manuzio[*],
P. Montagna[¶], H. Pruys[†], C. Regenfus[†], A. Rotondi[§§], G. Testera[*],
A. Variola[*], D. P. van der Werf[‡],
(ATHENA COLLABORATION)
and
R. L. Spencer[¶¶]

[*]INFN and Dipartimento di Fisica, Università di Genova, 16146 Genova, Italy
[†]Physik-Institut, Zürich University, CH-8057 Zürich, Switzerland
[**]EP Division, CERN, CH-1211 Geneva 23, Switzerland
[‡]Department of Physics, University of Wales Swansea, Swansea SA2 8PP, UK
[§]Instituto de Fisica, Universidade Federal do Rio de Janeiro, Rio de Janeiro 21945-970, and
Centro Federal de Educação Tecnologica do Ceara, Fortaleza 60040-531, Brazil
[¶]INFN and Dipartimento di Fisica Nucleare e Teorica, Università di Pavia, 27100 Pavia, Italy
[‖]Department of Physics, University of Tokyo, Tokyo 113-0033, Japan
[††]Department of Physics and Astronomy, University of Aarhus, DK-8000 Aarhus C, Denmark
[‡‡]Dipartimento di Chimica e Fisica per l'Ingegneria e per i Materiali, Università di Brescia and
INFN (Gruppo collegato di Brescia), 25123 Brescia, Italy
[§§]INFN and Dipartimento di Fica Nucleare e Teorica, Università di Pavia, 27100 Pavia, Italy
[¶¶]Department of Physics and Astronomy, Brigham Young University, Provo, Utah 84602

Abstract. Production of antihydrogen atoms by mixing antiprotons with a cold, confined, positron plasma depends on parameters such as the plasma density and temperature. We discuss a non-destructive diagnostic, based on an analysis of excited, low-order plasma modes, that provides comprehensive characterization of the positron plasma in the ATHENA antihydrogen apparatus. The dipole and quadrupole modes of a spheroidal positron plasma are interpreted in the framework of a cold fluid theory. In particular, the excitation and detection of the dipole mode are analytically modeled considering the response of the center-of-mass to a resonant driving perturbation. The model is compared to, and validated by, numerical simulations with a particle-in-cell code. Measurements of the positron plasma properties are discussed.

---

[1] Corresponding author (marco.amoretti@ge.infn.it)

INTRODUCTION

Recently cold antihydrogen atoms where produced in the ATHENA experiment (**A**ppara**T**us for **H**igh precision **E**xperiments on **N**eutral **A**ntimatter, or shortly **A**n**T**i**H**ydrog**EN A**pparatus) at CERN (European Organization for Nuclear Research) by mixing low energy antiprotons with a cold dense positron plasma inside an electromagnetic trap [1].

Very low positron and antiproton temperatures (a few K) and high positron density ($\simeq 10^8$ particles/cm^3) are the two key ingredients necessary to enhance the recombination rate in ATHENA. Under these conditions the positron cloud is in the plasma regime. In order to understand and control the recombination process, several parameters describing the positron plasma in thermal equilibrium should be measured in a non-destructive way to avoid perturbing the system.

Harmonically confined one component plasmas at temperatures close to absolute zero take the shape of an ellipsoid characterized by an aspect ratio $\alpha = z_p/r_p$, where z_p and r_p are the semi-major axis and semi-minor axis respectively. A simple analytic model for low-order axisymmetric plasma modes (Trivelpiece-Gould modes) in a spheroidal plasma has been used as a diagnostic in the ATHENA experiment [2, 3], where these modes were excited and detected to gain information about the positron plasma. The two lowest-order (dipole and quadrupole) modes were interpreted in the framework of a cold fluid theory [4]. The mode frequencies depend only on the plasma density n and aspect ratio α. Corrections due to finite temperature have also been calculated [5, 6]. Previous studies [6, 7, 8, 9, 10, 11, 12, 13] have extracted the information contained in the mode frequencies themselves. The plasma density and aspect ratio can be derived by comparing the measured frequencies of the dipole and quadrupole modes with those predicted by theory. But the actual plasma length and radius (or, equivalently, the number of particles) cannot be ascertained by using only frequency data. However, in Ref. [3], we demonstrated that the plasma length can be extracted from a detailed analysis of the power transmitted through the plasma near the resonance of the center-of-mass mode.

The model described in Ref. [3] can be numerically validated using a non-neutral plasma equilibrium code EQUILSOR [14] coupled with a two-dimensional ($r - z$) particle-in-cell (PIC) simulation RATTLE [6]. The first code (EQUILSOR) is dedicated to the evaluation of the plasma thermal equilibrium. The code solves the Poisson-Boltzmann equilibrium equation assuming axisymmetry [15]. The second code (RATTLE) uses the computed equilibria to create initial distributions of particles in (r, z, v_z)-space and then simulates the motion of the particles via a standard PIC technique. The same numerical codes were used by Surko and co-workers [6] to investigate the applicability of Dubin's mode theory [4] to their electron plasma.

This paper is organized in the following manner. The following section briefly describes the experimental setup. The third section is a concise review of the model used to describe the center-of-mass (dipole) mode and confirms its validity by means of a comparison with numerical simulations. In the fourth section a possible extension of the model in order to study the plasma response for the quadrupole mode is discussed. The simulation results show that the extension developed in Ref. [3] also works for the quadrupole mode. The concluding section presents an example of the application of the diagnostic.
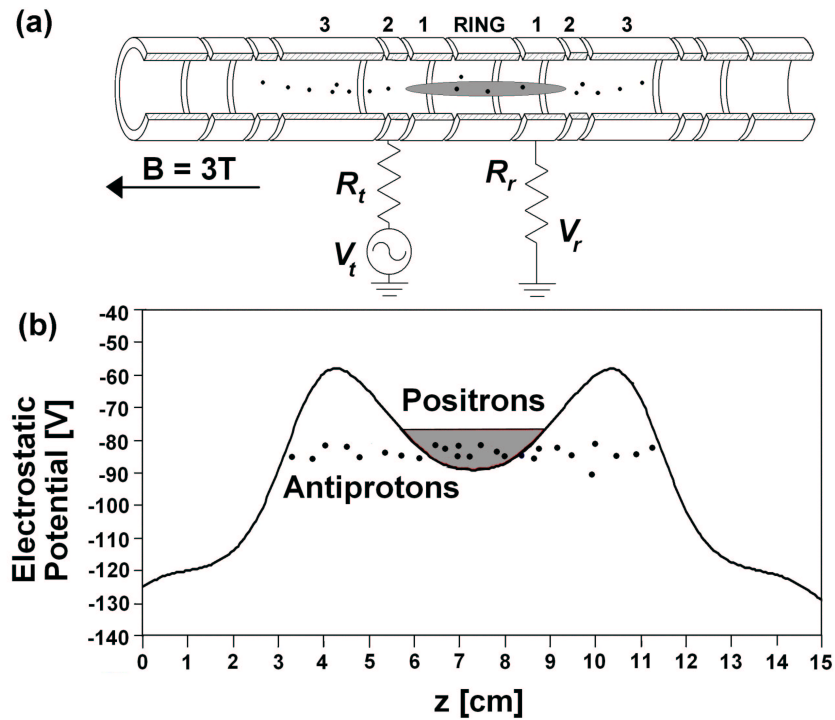
FIGURE 1. (a) Schematic of the mixing trap electrodes. The positrons are confined in the center group designed to create a harmonic electrostatic field. The central electrode is called the ring electrode and the other 3 pairs are labeled 1, 2 and 3. The driving signal applied to one electrode is shown together with the resistances on the transmitting and receiving electrodes. The shape of the prolate positron ellipsoid is shown schematically. (b) The axial potential of the ATHENA nested trap is shown and the ranges of axial motion of the positrons and of the antiprotons is indicated schematically.

EXPERIMENTAL SETUP

Electromagnetic traps of the Penning-Malmberg type are used in the ATHENA experiment to confine charged particles. The traps are realized by placing a series of cylindrical electrodes of various lengths and with an inner radius of 1.25 cm inside a uniform 3-Tesla magnetic field parallel to the trap axis and applying static voltages to them. A potential well along the trap (or $z-$) axis is thereby produced which provides axial confinement for particles having energies lower than the top of the well. The magnetic field ensures radial confinement. The trap structure is installed inside a cryogenic bore and can be cooled to about 15 K. The voltages on these electrodes are manipulated to perform various procedures.

The mixing trap [Fig. 1(a)] is composed of 3 groups of electrodes which produce the nested trap configuration [Fig. 1(b)]. Thus, the simultaneous confinement of particles having opposite signs of charge is achieved. The positron confining region is comprised of seven electrodes. The lengths of these electrodes have been chosen, according to Ref. [16], in order to create a harmonic potential when the ratios between the applied voltages are suitably chosen.

The axial modes are excited by applying a sinusoidal perturbation to one electrode

with an electromotive force $V_t = v_t e^{j\omega t}$. The resulting oscillation of the plasma induces a current in the pick-up electrode [17, 18, 19] and a voltage $V_r = v_r(\omega)e^{j\omega t}$ is detected across the resistance R_r [Fig. 1(a)].

DIPOLE MODE

In cold fluid theory [4], the lowest-order mode is a coherent oscillation of the whole plasma along the z axis with a frequency ω_1 equal to that of single particle motion inside the trap,

$$\omega_1 = \omega_z = \sqrt{\frac{qV_0}{md^2}}. \tag{1}$$

In Eq. (1) q is the particle electric charge and m is its mass, V_0 is the potential difference between the ring and the type 3 electrode, and the length d is related to the trap radius r_w ($d = 1.74\, r_w$ for the mixing trap design).

A simple model, based on the observation that the dipole mode can be described as a damped oscillation of the center-of-mass of the positron cloud, enables study of the excitation and detection processes. The center-of-mass equation of motion along the trap axis can be written as [3]:

$$\ddot{z}_{cm} + \gamma\dot{z}_{cm} + \omega_1^2 z_{cm} = \frac{q}{m}\langle E_{zi}\rangle, \tag{2}$$

where z_{cm} is the axial position of the cloud center-of-mass and γ describes the damping of the oscillations. In this equation the driving term $\langle E_{zi}\rangle$ is an effective axial electric field acting on the center-of-mass when a potential V_i is applied on the electrode labeled i (i indicates the electrode type, see also Fig. 1(a)). It can be approximated by

$$\langle E_{zi}\rangle = g_i(\alpha, z_p)\frac{V_i}{2r_w}, \tag{3}$$

where the characteristic function $g_i(\alpha, z_p)$, defined by

$$g_i(\alpha, z_p) = \frac{3\alpha^2 r_w}{z_p^3}\int_{-z_p}^{z_p} dz \int_0^{z_p\alpha^{-1}\sqrt{1-z^2/z_p^2}} rdr F_{zi}(r,z), \tag{4}$$

has been introduced to describe the coupling between the perturbation signal and the center-of-mass response. In Eq. (4), $F_{zi}(r,z)$ represents the axial component of the electric field at the position (r,z) when a unit potential is applied on the electrode i while the rest of the electrodes are grounded. The factor $g_i(\alpha, z_p)$ can be numerically evaluated using a truncated Fourier-Bessel series (as in Ref. [3]) or by using directly the EQUILSOR-RATTLE numerical Poisson solver. This coupling function depends not only on the trap geometry and on the type of the electrode used to drive the mode, but also on the size and shape of the plasma. It has a strong dependence on the plasma length, but only weakly depends on the aspect ratio (or, equivalently, on the plasma radius; see Fig. 2).
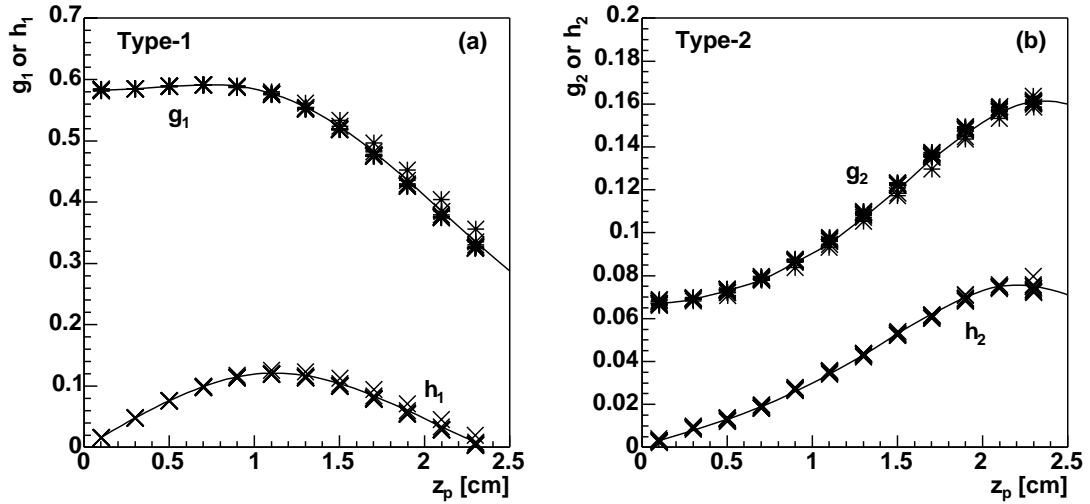
FIGURE 2. Dependence of the characteristic functions describing the coupling between the perturbation signal and dipole (g_i) and quadrupole (h_i) modes on the plasma semi-length for (a) type-1 and (b) type-2 electrodes (see the discussion in the text). The values are evaluated using the EQUILSOR-RATTLE numerical Poisson solver. The scattering of the points reflects the dependence on the aspect ratio. The solid curves are for aspect ratio $\alpha = 6$.

This model allows estimation of the growth of the mode due to the application of a sinusoidal perturbation to one transmitting electrode [$i = t$, see also Fig. 1(a)]. If we suppose that the driving frequency is in perfect resonance with the natural frequency of this mode, i.e., $V_t \sin \omega_1 t$, then the velocity of the center-of-mass, $\dot{z}_{cm}$, is characterized by a linear growth with an acceleration

$$a_{cm} = g_t(\alpha, z_p) \frac{qV_t}{4mr_w}. \tag{5}$$

To test the accuracy of this simple model, the excitation process was directly simulated using EQUILSOR-RATTLE. First, a series of thermal equilibria characterized by the same plasma radius, but with different numbers of particles N and plasma half-lengths z_p, were generated. The plasmas were confined in the central part of the nested trap configuration with electrode potential values equal to those used in the mixing studies in the ATHENA experiment. The exciting perturbation was applied in separate runs to both type-1 and type-2 electrodes. The simulated growth rates were then compared with the rates predicted by Eq. (5). Figure 3 shows the good agreement between the simulation and the model.

The coupling function $g_r(\alpha, z_p)$ also allows estimation of the induced current on a single electrode due to the center-of-mass oscillation. Following the model, the current induced on the receiving electrode [labeled by r, see also Fig. 1(a)] is given by Eq. (19) of Ref. [3], i.e.,

$$I_r = g_r(\alpha, z_p) \frac{qN}{2r_w} \dot{z}_{cm}. \tag{6}$$
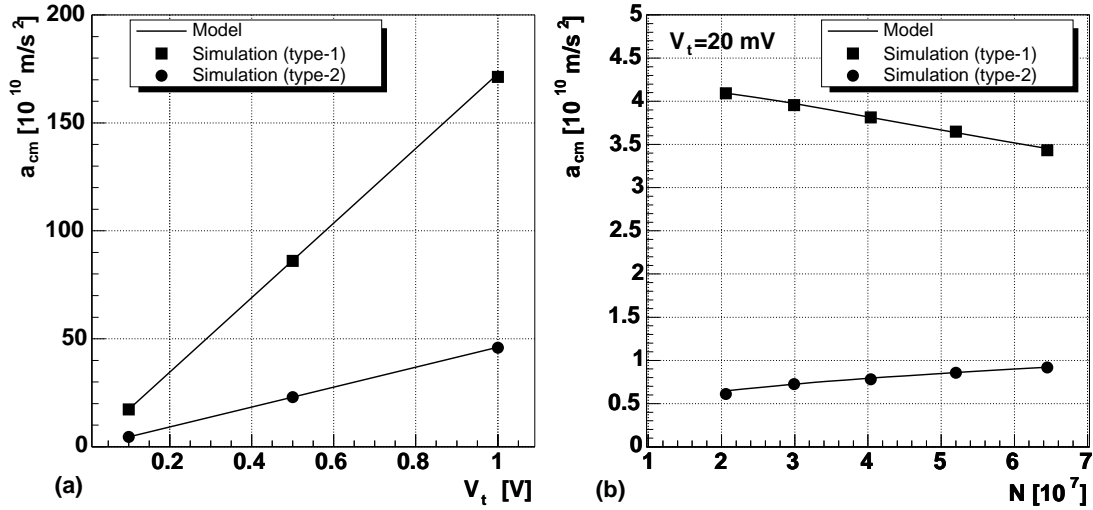
FIGURE 3. (a) Dependence of the acceleration amplitude a_{cm} of the center-of-mass oscillation on the amplitude of the perturbation V_t applied in resonance with ω_1. The time duration of the perturbation is limited to a few cycles of the dipole oscillation. Otherwise, for $V_t > 0.1$ V saturation effects are soon visible. The plasma was characterized by $z_p = 1.63$ cm, $r_p = 0.22$ cm, $n = 2 \times 10^8$ cm^{-3}, and temperature $T = 0.1$ meV. (b) Acceleration amplitudes a_{cm} of the center-of-mass oscillation for different plasmas subjected to an external sinusoidal perturbation $V_t \sin \omega_1 t$ applied on a type-1 or type-2 electrode. The simulated plasmas are characterized by different values of particle number N and axial semi-length z_p but they have all the same radius $r_p = 0.22$ cm. In both (a) and (b) the solid lines are the growth rates evaluated using Eq. (5).

If the maximum of the oscillation is z_{offset} then

$$I_r = g_r(\alpha, z_p) \frac{qN}{2r_w} \omega_1 z_{\text{offset}}. \tag{7}$$

The simplest way to test the validity of this relation is to simulate the oscillation of the center-of-mass by giving an axial offset z_{offset} to all of the plasma particles in RATTLE. The simulated current is obtained by numerically integrating the normal component of the electric field over the electrode under consideration, then numerically differentiating this charge as a function of time to find the current. Figure 4 shows the comparison between the analytic model and the simulation and, again, the agreement is very good (the relative difference between the simulations and our analytic model is less than 1%).

QUADRUPOLE MODE

The quadrupole mode frequency ω_2 can be evaluated using the dispersion relation of the axisymmetric modes in a cold fluid spheroid [4, 6], i.e.,

$$1 - \frac{\omega_p^2}{\omega_2^2} = \frac{k_2}{k_1} \frac{P_2(k_1) Q_2^{0'}(k_2)}{P_2'(k_1) Q_2^0(k_2)} \tag{8}$$
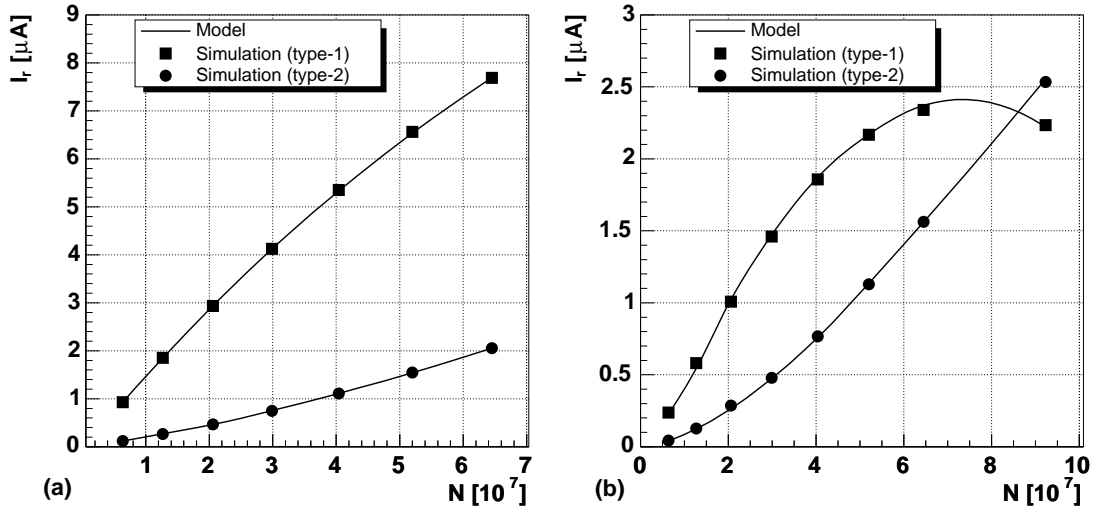
FIGURE 4. (a) Simulated induced current on the trap electrodes due to the oscillation of the center-of-mass for different plasmas ($z_{\text{offset}} \simeq 0.3$ mm). The solid lines represent the values of the induced currents evaluated by means of Eq. (7). (b) Simulated induced current on the trap electrodes due to the quadrupole mode for different plasmas ($z_{\text{stretch}} \simeq 0.3$ mm). The solid lines represent the values of the induced currents evaluated by means of Eq. (10).

where P_2 is a Legendre polynomial, Q_2^0 is its singular partner, $\omega_p = \sqrt{nq^2/\varepsilon_0 m}$ is the plasma frequency, $k_1 = \alpha/\sqrt{\alpha^2 - 1 + \omega_p^2/\omega_2^2}$, and $k_2 = \alpha/\sqrt{\alpha^2 - 1}$.

The model developed for the evaluation of the center-of-mass excitation and detection can be extended in order to describe the quadrupole mode oscillations. The extension is based on the introduction of coupling factors $h_i(\alpha, z_p)$ similar to the functions $g_i(\alpha, z_p)$ described above. In this case the coupling functions reflect the "stretching nature" of the quadrupole mode,

$$h_i(\alpha, z_p) = \frac{3\alpha^2 r_w}{z_p^3} \int_{-z_p}^{z_p} dz \frac{z}{z_p} \int_0^{z_p \alpha^{-1} \sqrt{1 - z^2/z_p^2}} r dr F_{zi}(r, z). \tag{9}$$

Figure 2 shows a comparison between $g_i(\alpha, z_p)$ and $h_i(\alpha, z_p)$ values.

Using the factors $h_r(\alpha, z_p)$ evaluated for the receiving electrode, a relationship similar to that of Eq. (6) can be written:

$$I_r = h_r(\alpha, z_p) \frac{qN}{2r_w} \omega_2 z_{\text{stretch}}, \tag{10}$$

where $\omega_2 z_{\text{stretch}}$ can be identified as the maximum velocity of the particles in the plasma due to the oscillation of the mode.

An antisymmetric linear stretch of the plasma along the z axis is used to excite the quadrupole mode in the simulations. Despite the simplicity of Eq. (10) the agreement between the simulation results and the model predictions is good (see Fig. 4).

EXPERIMENTAL RESULTS

The experimental implementation of this diagnostic is extensively discussed in Ref. [3]. In this section an example of monitoring the plasma parameters during a long period of evolution is shown. In these measurements a plasma of about 4×10^7 positrons was confined in the nested trap for about 1000 s without the injection of antiprotons.

The number density and aspect ratio were extracted using the measured frequencies (ω_1, ω_2) of the dipole and quadrupole modes and combining equations (1) and (8). The evolution of these two parameters during the plasma expansion is shown in Fig. 5.

For a complete non-destructive diagnostic it is necessary to measure another parameter: the total number of particles N, or either r_p or z_p ($N = 4\pi n z_p^3/3\alpha^2 = 4\pi n\alpha r_p^3/3$). None of these quantities can be determined by using the frequency data even if higher order longitudinal modes are detected. But the missing parameter can be extracted by a complete study of the way the plasma mediates the transmission of a driving signal on one electrode to a different receiving electrode. The signal transmitted through the plasma for a driving frequency near ω_1 is characterized by a resonance shape. Using the model discussed in the previous sections it is possible to approximate the plasma response to that of a resonant RLC circuit to an external drive. The parameters of the resulting circuit depend on all of the plasma properties, so that the shape of the resonant response makes it possible to evaluate these parameters, and consequently the remaining plasma properties. Figure 6 shows the time evolution of the plasma length and radius, while the reconstructed number of positrons obtained from the resonance curve is shown in Fig. 7(a). The fluctuations in the data are mainly due to the experimental signal-to-noise ratio of the quadrupole mode signal. Improving the signal-to-noise ratio by increasing the mode driving amplitude would, however, result in an unfavorable plasma heating effect.

An example of the application of this diagnostic to positrons during antihydrogen
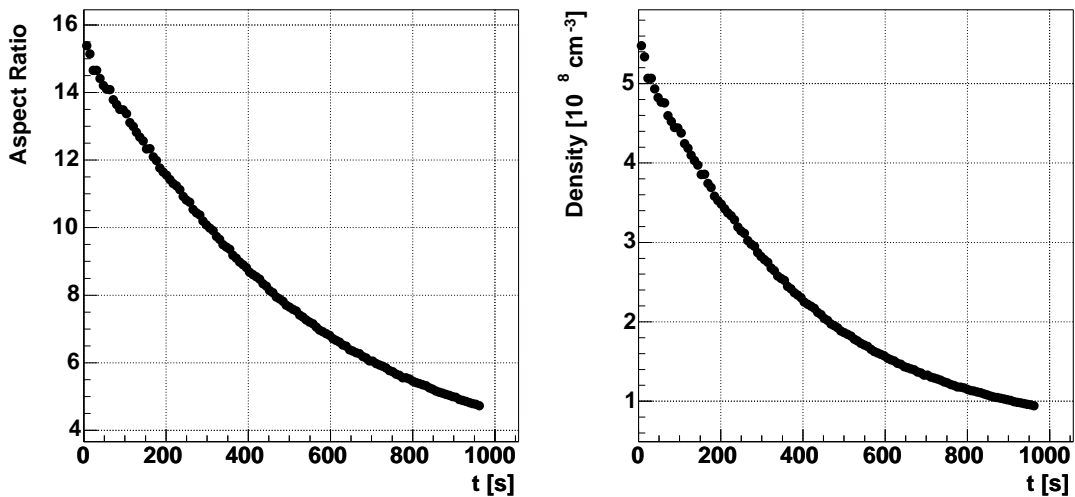
FIGURE 5. The evolution of the aspect ratio and the number density for a plasma of about 4×10^7 positrons confined in the nested trap for about 1000 s without the injection of antiprotons.
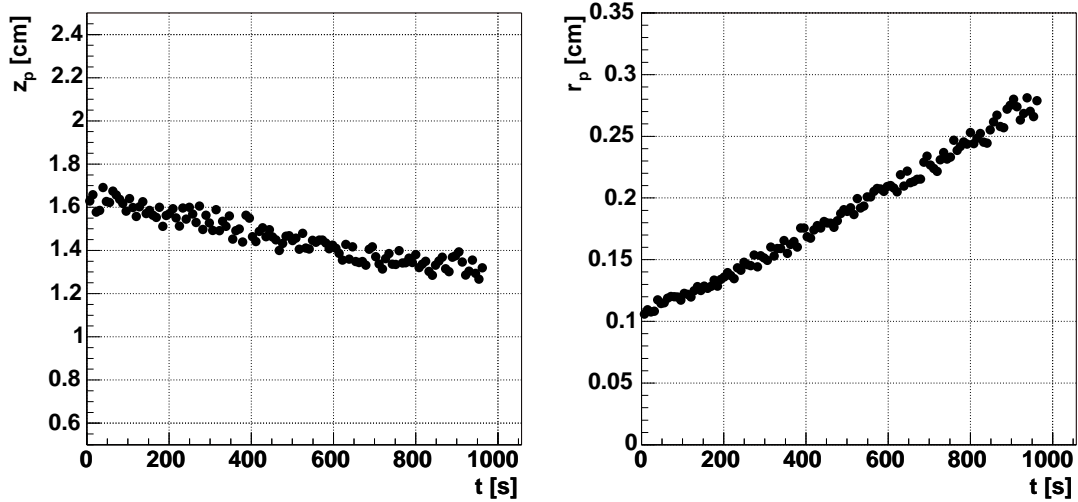
FIGURE 6. The evolution of the plasma semi-length and radius for the same plasma as Fig. 5.
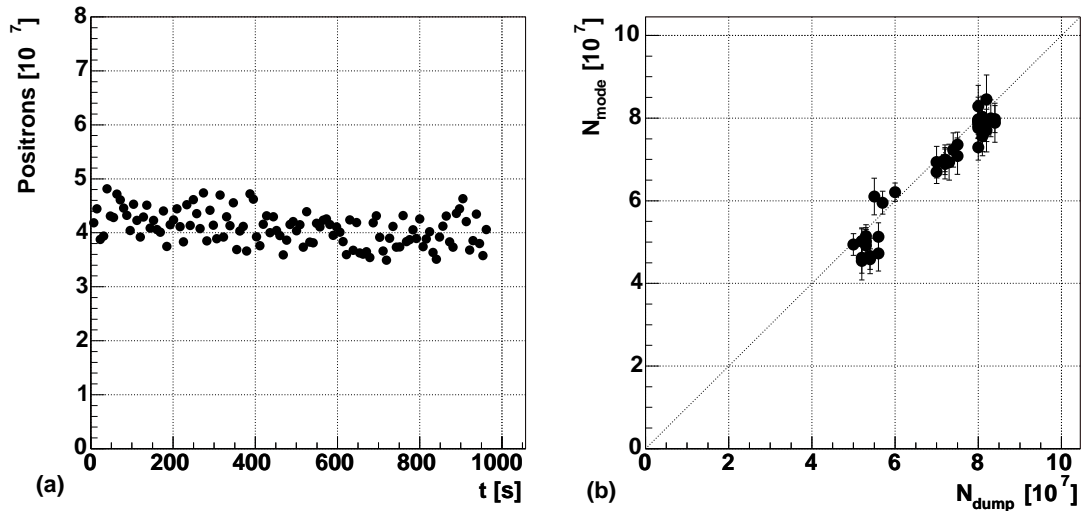
FIGURE 7. (a) Total number of positrons estimated by means of the transmission diagnostic for the plasma evolution of Fig. 5. (b) The total number of positrons obtained by using the transmission diagnostic is plotted against the number obtained by extracting the positrons to a Faraday cup.

production is shown in Fig. 7(b). Here the total number obtained by using the model is plotted against the number found by extraction to a Faraday cup. In this regime the linearity and good correspondence in the absolute number show that both the model and its implementation constitute a complete non-destructive plasma diagnostic. Typical measured properties of the ATHENA positron plasma for antihydrogen production were 7×10^7 positrons at a density of about 1.7×10^8 cm^{-3} in a plasma approximately 3.2 cm long ($2z_p$) with a radius of about 0.25 cm and a storage time of many hundreds of seconds.

CONCLUSION

We have extended the plasma mode diagnostic method to provide comprehensive characterization of the cold, dense positron plasma employed in the ATHENA antihydrogen experiment. The method has already been utilized to great advantage in ATHENA, and promises to be an essential element of future experiments. The technique, while particularly useful for non-destructive measurements on difficult-to-produce species such as positrons, has immediate applicability to other Penning trap plasmas.

ACKNOWLEDGMENTS

REFERENCES

1. M. Amoretti, *et al.*, Nature (London) **419**, 456 (2002).
2. M. Amoretti, *et al.*, Phys. Rev. Lett. **91**, 055001 (2003).
3. M. Amoretti, *et al.*, Phys. Plasmas. **10**, 3056 (2003).
4. D. H. E. Dubin, Phys. Rev. Lett. **66**, 2076 (1991).
5. D. H. E. Dubin, Phys. Fluids B **5**, 295 (1993).
6. M. D. Tinkle, R. G. Greaves, C. M. Surko, R. L. Spencer, and G. W. Mason, Phys. Rev. Lett. **72**, 352 (1994).
7. D. J. Heinzen, J. J. Bollinger, F. L. Moore, W. M. Itano, and D. J. Wineland, Phys. Rev. Lett. **66**, 2080 (1991).
8. J. J. Bollinger, D. J. Heinzen, F. L. Moore, W. M. Itano, D. J. Wineland, and D. H. Dubin, Phys. Rev. A **48**, 525 (1993).
9. C. S. Weimer, J. J. Bollinger, F. L. Moore, and D. J. Wineland, Phys. Rev. A **49**, 3842 (1994).
10. M. D. Tinkle, R. G. Greaves, and C. M. Surko, Phys. Plasmas **2**, 2880 (1995).
11. H. Higaki and A. Mohri, Jpn. J. Appl. Phys. Part 1 **36**, 5300 (1997).
12. T. B. Mitchell, J. J. Bollinger, X.-P. Moore, and W. M. Itano, Optics Express **2**, 314 (1998).
13. H. Higaki, N. Kuroda, T. Ichioka, K. Yoshiki Franzen, Z. Wang, K. Komaki, Y. Yamazaki, M. Hori, N. Oshima, and A. Mohri, Phys. Rev. E **65**, 046410 (2002).
14. R. L. Spencer, S. N. Rasband, and R. R. Vanfleet, Phys. Fluids B **5**, 4267 (1993).
15. S. A. Prasad and T. M. O'Neil, Phys. Fluids **22**, 278 (1979).
16. H. Raimbault-Hartmann, D. Beck, G. Bollen, M.König, H.-J. Kluge, E. Schark, J. Stein, S. Schwarz, J. Szerypo, Nucl. Instr. and Meth. **B 126**, 378 (1997).
17. M. D. Sirkis and N. Holonyak, Am. J. Phys. **34**, 943 (1966).
18. C. A. Kapetanakos and A. W. Trivelpiece, J. Appl. Phys **41**, 4841 (1971).
19. D. J. Wineland and H. G. Dehmelt, J. Appl. Phys **46**, 919 (1975).